

**Examination of Contacts Between Strands by Electrical Measurement
and Topographical Analysis**

J-M. Depond, D. Leroy, L. R. Oberli and D. Richter

Abstract

The contact resistance (crossing and adjacent) between the strands of Rutherford type superconducting cables has been proven to be an essential parameter for the behaviour of the main magnets in accelerators like the LHC. A strong development program has been launched at CERN.

Contact resistances were measured by means of a DC method at 4.2 K.

The strand deformation and the chemical conditions at the contacts were analyzed in order to interpret the electrical resistances measured by a 3 contacts method on individual strands as well as the resistances measured independently on cables.

LHC Division

ASC Pittsburg '96

Administrative Secretariat
LHC Division
CERN
CH - 1211 Geneva 23
Switzerland

Geneva, 30 October 1996

Examination of Contacts Between Strands by Electrical Measurement and Topographical Analysis

J-M. Depond, D. Leroy, L. R. Oberli and D. Richter
CERN, CH-1211 Geneva 23, Switzerland

Abstract—The contact resistance (crossing and adjacent) between the strands of Rutherford type superconducting cables has been proven to be an essential parameter for the behaviour of the main magnets in accelerators like the LHC. A strong development program has been launched at CERN.

Contact resistances were measured by means of a DC method at 4.2 K.

The strand deformation and the chemical conditions at the contacts were analyzed in order to interpret the electrical resistances measured by a 3 contacts method on individual strands as well as the resistances measured independently on cables.

I. INTRODUCTION

In the framework of the R&D program on the LHC superconducting cable [1], interstrand contacts have been analysed for the dipole inner layer cable. Based on theoretical and experimental considerations, their electrical resistance has to be higher than 10-20 $\mu\Omega$ in order to limit especially the dynamic field errors. Several research lines are followed in order to reach this value: measurements in magnet coils [2], measurements in industrially made cables [1] and measurements on strands with various coatings. For this last way, we have implemented a 3 contacts device, measuring the relationship between the contact resistance R_c and the loading force. This gives us not only a good understanding of the mechanisms which influence R_c , but also a first estimation of R_c in the LHC cables made with such superconducting strands.

After presenting some properties of the contacts in LHC cables, we describe the 3 contacts experiment and the selected industrial coatings. We then analyse R_c measurements for these coatings. Finally, we correlate these results with the measurements made on equivalent cables and discuss the validity of some possible extrapolations.

II. CONTACT PROPERTIES

A. Strand and cable descriptions

The LHC superconducting strand is a composite structure [3] consisting of a pure Cu core surrounded firstly by a ring of NbTi filaments twisted and embedded in a Cu matrix and then covered by a Cu layer. A 1 μm thick coating layer is deposited on the outer surface by hot dipping or electrochemical plating. The final diameter is 1.065 mm.

The cable is made of 28 superconducting strands transposed with a pitch of 115 mm. The trapezoidal shape of

the cable is obtained by passing the strands through a turk's head where local loading pressures estimated at 750 N/mm² strongly deform the strands. At each strands crossing, an elliptic area of deformation is formed which fixes R_c . After cabling, the lateral surface of the strands is flat.

B. Mechanical behaviour and contact geometry

The high loading forces required by the cable fabrication or applied in the 3 contacts experiment, described below, deform the strands plastically. The mechanical contact area S is then defined by the ratio of the load F to the wire hardness H . Fig. 1 shows the hardness calculated from measurements of S versus the load F . In the strands, H varies from low values, due to the soft Cu, to high values, due to the hard NbTi filaments and becomes constant at a load of 90 N.

In the cable, the contact surface has a saddle shape. Fig. 2 presents the measured contact area along a strand over half a twist-pitch of a cable [4]. The area increases from the thick edge to the thin edge of the cable and has a mean value of 1.25 mm². In most of the 3 contacts experiments, the deformation is close to be circular because the wires crosses at 90° and the loading force is small. The maximum area so created is 10 times smaller than in a cable.

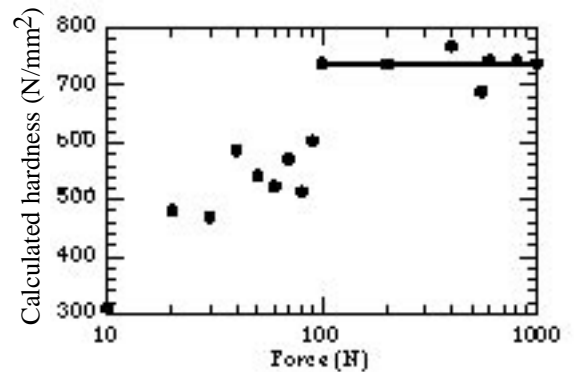


Fig. 1. Hardness versus loading force in a superconducting strand.

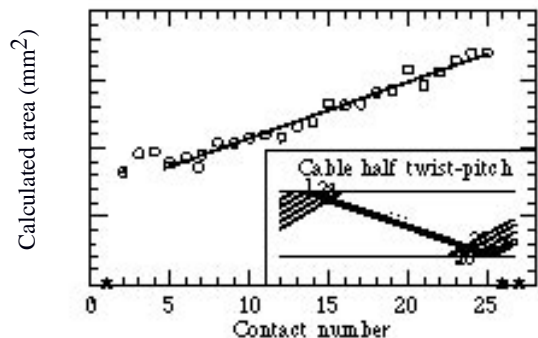


Fig. 2. The contact area along a strand over half a twist-pitch.

C. Electrical contact behaviour

According to Holm's theory [5], the contact resistance R_c is

$$R_c = 2R_{Super}^{Cu} + 2 \frac{\rho_{Cu}^e Cu}{S} + \frac{\rho_{Cu}}{2a} + 2 \frac{\rho_{Co}^e Co}{S} + 2 \frac{\rho_{OxeOx}}{S}. \quad (1)$$

where ρ_{Cu} (ρ_{Co} , ρ_{Ox} resp.) is the electrical resistivity of the outer Cu layer (coating, surface oxides resp.), e_{Cu} , (e_{Co} , e_{Ox} resp.) its thickness (coating, surface oxides resp.) and a the equivalent contact radius. $2R_{Super}^{Cu}$ is the resistance due to the superconducting to normal transfer from the NbTi filaments to the Cu layer. The second term is the Cu layer resistance. The third term is the constriction resistance due to the deformation of the current lines inside the Cu layer across the contact. The last two terms represent the coating resistances, including the surface oxide effect. Terms #1, #2 and #4 are usually much smaller than the others and are neglected. The fifth term, which usually governs the contact resistance, is difficult to calculate due to the uncertainty of the chemical composition of the coating.

In the present cable geometry, the contact area between two strands is larger than the strand cross-section, and the constriction resistance becomes negligible.

III. EXPERIMENTAL SETUP

A. Experimental device

We have constructed a crossed wires device working at 4.2 K (Fig. 3). The total force of a compressed spring at room temperature is transmitted to the samples by a steel rod. It is equally distributed by a kneecap device between the three cold contacts. The force applied on each contact can be varied from 5 N to 100 N.

Two contact geometries can be implemented. One, with wires crossing at 90° , is used to compare R_c of the various studied coatings. The total force F_T is applied at 4.2 K on undeformed wires in a cycle from 20 N to 285 N and back to 20 N (7 N to 95 N back to 7 N per contact) with 1 N of

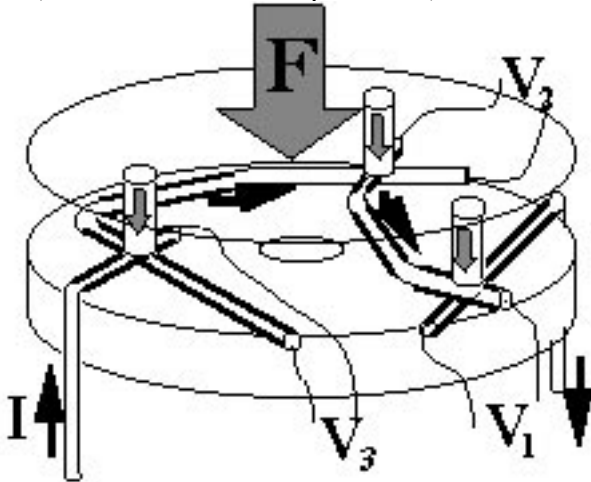


Fig. 3. Sketch of the 3 contacts experimental device

accuracy. The maximum circular deformation of each contact area is measured after the experiment. The second geometry, with wires crossing at 30° , is closer to the cable geometry and is used to compare R_c as measured in both the cable and wire experiments. A total load of 3000 N on the three contacts, which is applied at room temperature in an external press, causes areas of plastic deformation similar to the ones observed on cables. Deformed wires are then transferred to the sample holder, in a tool immobilizing the contacts. After cooling, R_c is measured under F_T values from 20 N to 285N.

All samples are cleaned by passing them through two acetone and one ethanol baths at room temperature.

The voltages V_1 , V_2 , V_3 on the contacts are measured using a Keithley 182 nanovoltmeter at currents I from 100 mA to 300 mA. In case of high resistive contact, I is reduced to 1 mA to 3 mA to avoid any Joule heating.

B. Tested samples

Table I presents the tested samples. Several coatings (SnAg, Ni, Zn, SnNi, ZnNi) have been deposited on the same virgin wire. Only industrially processable coatings have been selected.

SnAg has been the most studied because it can be easily deposited at high speed by hot dipping. It has been chosen for its low Kapitza resistance at 1.9 K. Its mechanical properties like adherence and ductility are good. We have studied samples coming from different fabrications: samples BA2 and B98 have been coated after final drawing to the nominal strand diameter; samples BC2 and B63 have been drawn to the nominal diameter after coating.

Nickel is industrially electrochemically plated. Numerous cracks are observed under pressure. Due to the presence of a surface oxide layer, soldering needs special care.

Zinc is also industrially deposited by electromechanical plating with high speed. Mechanical and soldering properties are good but the coating is highly sensitive to humidity. We have observed the creation of hydroxides and degradation of the coating. The chemical passivation by chromium compounds produces a glassy transparent protective layer.

TABLE I

TESTED COATINGS AND WIRES

Ref.	Coating	Deposition Mode	Remark
BA	SnAg _{5%w}	Hot dipping	Reference wire for
BC	SnAg _{5%w}	Hot dipping	Twisting and drawing
B98	SnAg _{5%w}	Hot dipping	1.098 mm diameter
B63	SnAg _{5%w}	Hot dipping	B98 after drawing to
	SnNi	Electrochemical	
	Ni	Electrochemical	
	Ni +	Plating	0.8 μ m
	NiP _{13%w}		0.2 μ m (chemical)
	ZnNi	Electrochemical	
	Zn	Electrochemical	
	Passived Zn	Electrochemical	Chemical passivation
	Oxidized Cu		Chemical oxidation

SnNi and ZnNi have also been produced by electrochemical deposition.

The oxidized uncoated strand has been chemical oxidation.

IV. RESULTS

After analysing a typical R_c versus F_T curve, we compare the behaviour of the tested coatings. We also correlate some data to the equivalent measurements on cable and establish a possible extrapolation.

A. Contact resistance versus loading force

Fig. 4 shows a typical curve obtained by the 3 contacts experiment. The tested samples are BA2 wires with SnAg coating. F_T , applied on the three contacts, is reported on the X axis and measured R_c on the Y axis. Empty circles correspond to data when F_T is increased from 20 N to 285 N and filled circles when F_T is decreased from 285 N to 20 N. The dotted curve is a best fit of the F_T increasing cycle according to (1).

Considering increasing F_T , R_c decreases when F_T increases in a different way as given by (1). This can be due to:

i) The force distribution which can vary between the three contacts when F_T increases. We measure the maximum deformation areas after each experiment to have the exact distribution at the highest load.

ii) The hardness which is an important parameter in (1). Its relation versus applied force is complex and known only by measurements. We are not sure that this relation is valid for each sample.

iii) The plastic phenomena such as oxide layer breaking and creep which are not taken into by (1). Due to these phenomena, we have observed a "cleaning effect": samples with very different R_c values at low force (probably due to different states in their surface oxidation) converge towards similar values at high force. Confirming this hypothesis, we observe a better agreement with gold coated samples where no oxidation phenomena occur.

Considering decreasing F_T , R_c remains constant when F_T decreases from 285 N down to 80 N. Below 80 N, a fast increase of R_c is observed. A possible explanation is that, in the composite structure of the wire, when the applied force

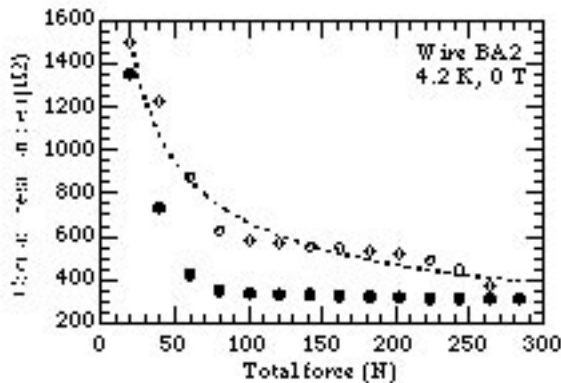


Fig. 4. The contact resistance as function of the total loading force for force increasing and decreasing cycles.

decreases, the hard material starts to relax following an elastic behaviour. Its high Young's modulus involves a really small displacement which is absorbed by the soft material above without changing the contact geometry. Below a certain force, the soft material can not absorb any bigger displacement and the contact area starts to reduce fast.

B. Contact resistance for different coatings

Using the 3 contacts experiment data, we have established some criteria to compare contact resistances of samples with different coatings. We consider the value measured for the highest total applied force (285 N) multiplied by the contact area, taking into account the effective load on each contact. It is called equivalent R_c .

Statistical data are reported in Fig. 5 for all the studied samples. The tick is the median (50% probability) of the 6 to 9 measurements per sample and the vertical line is the 25%-75% spread of the statistical distribution. We have to remark that a spread of half an order of magnitude is common in R_c measurements, especially when the surfaces are oxidized. Moreover, the spreads are amplified by the small number of measured data. Several observations can be made:

1) *Drawing effect*: In both the cases (BA2/BC2, B98/B63), we observed an increase in equivalent R_c . A possible explanation is the increase of the surface oxide thickness due to the breaking and the sinking of the pre-existent oxide layer inside the coating layer during the drawing and the creation of new oxides on the cleaned surface.

2) *Heating effect*: We have observed a systematic effect due to some short heating during the mounting on the sample holder (shown as dots in Fig. 5). For SnAg coating, this causes a reduction of the equivalent R_c by a factor 2 to 8, whereas the factor is only 2 to 3 for SnNi and Ni coatings. For ZnNi and Zn coatings, we observe an increase of a factor 3 to 20. Heating usually induces some surface oxidation which increases the oxide thickness and hence the resistance,

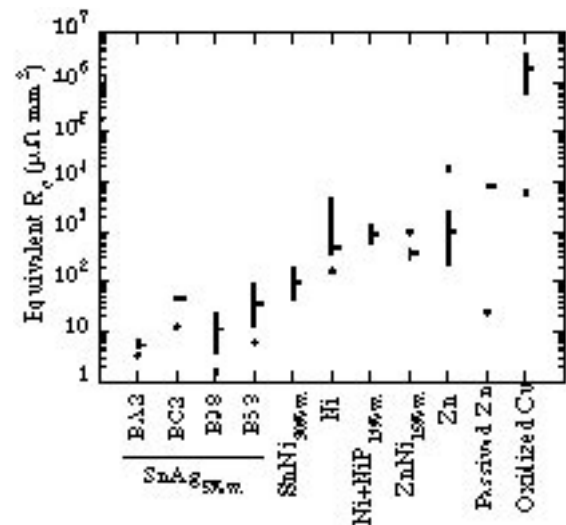


Fig. 5. Comparison of the equivalent contact resistance between various tested coatings.

but also some oxide diffusion inside the coating which decreases the oxide thickness and hence the resistance [6]. The predominance of one effect to the other can therefore explain our results.

3) *Oxide breaking effect*: Passivated Zn and oxidized Cu coatings show high equivalent R_c values due to the thick surface oxide layer. Nevertheless, we have measured extremely low resistance values (being a factor 300 smaller than the median value -see the dots in Fig. 5). In these cases, some important surface cracks and creeps are observed using an optical microscope with polarized light. This causes numerous metal/metal contacts through the oxide layer cracks which strongly decrease the equivalent R_c .

4) *Type of coating*: SnAg coating results in low equivalent R_c values ($\approx 10 \mu\Omega \text{ mm}^2$). Ni coating induces higher values ($\approx 500 \mu\Omega \text{ mm}^2$) increasing up to $\approx 1000 \mu\Omega \text{ mm}^2$ if a NiP layer is added. This can be explained by the difference in the coating hardness: the soft coating of SnAg creeps, so it is oxide-cleaned more easily than the hard coating of Ni where the oxide layer can only break. The behaviour of SnNi coating is somewhat in-between. Zn coating results in high equivalent R_c values ($\approx 1000 \mu\Omega \text{ mm}^2$). This value increases up to $\approx 9000 \mu\Omega \text{ mm}^2$ by passivation which adds an highly resistive layer on the surface. The adjunction of nickel decreases the contact resistance to $\approx 400 \mu\Omega \text{ mm}^2$, probably because Ni is preferentially oxidized in the Zn/Ni system and a thin NiO is created instead of the more resistive ZnO₂ layer [6]. Finally, chemical oxidized bare wire has the highest contact resistance values ($\approx 2 \Omega \text{ mm}^2$) due to the thick and highly resistive CuO₂ layer on the surface.

C. Strand to cable extrapolation

Knowing the average contact area for crossing contacts in a cable ($\approx 1.25 \text{ mm}^2$), we can try to estimate the R_c value in the cable by extrapolating equivalent R_c measured on wires at F_T equal to 285 N. Indeed, we have shown in Fig. 4 that R_c is equal, for a large range of loading force (F_T between 80 N and 285 N), to R_c reached for the maximum loading force ($F_T = 285 \text{ N}$). In the tested cables, the density of contacts per mm^2 is about 0.862 so that, under standard 50 MPa pressure, the force applied per crossing contact is about 58 N. This corresponds to F_T equal to 174 N in the 3 contacts experiment, high enough to validate the extrapolation.

We have verified the correlation with the value measured directly on a cable for samples BA2 and BC2 [1]. The results (Table II, col. 2-3) show that, using the 3 contacts method,

TABLE II

WIRE AND CABLE MEASUREMENTS				
Ref.	Coating	Extrapolated R_c (Wire)	Measured R_c (Cable)	Measured R_c (Deformed Wire at 182 N)
BA2	SnAg _{5%w.}	5.4 $\mu\Omega$	11-15 $\mu\Omega$	10 $\mu\Omega$
BC2	SnAg _{5%w.}	49 $\mu\Omega$	18-27 $\mu\Omega$	26 $\mu\Omega$

we are able to estimate and classify the R_c value on real cables with different coatings within an order of magnitude. A better estimation is probably not possible since the plastic deformation is stronger in a cable than in the 3 contacts experiment, so the creep is larger and the surface oxidation is different. Fig. 5 gives therefore only an order of magnitude for the R_c value in cables.

We have deformed some wire samples at high loading force and then measured in the 3 contacts experiment (see geometry 2 in section II.A). Results are reported in column 4 for 182 N total load during a force increasing cycle. The data are in good agreement with measurements on the cables and validate this kind of experiment for future measurements, which will include thermal treated wires.

V. CONCLUSION

To study the contact resistance of wires with various coatings, a 3 contacts measurement device at 4.2 K has been developed where the loading force can be varied from 5 N to 95 N per contact. In this range of force, the contacts show a plastic deformation and the R_c values are governed by the maximum applied force and the physical state of the surface layer. Experiments on wires deformed at higher loading force ($\approx 1000 \text{ N}$) give contact areas similar to the ones measured in cables. The work for classifying industrially coated strands has started in order to preselect the coatings for the LHC strands. First information about the role of the oxides to reach the wanted value (20 $\mu\Omega$) of R_c for the LHC machine has been obtained. Implementing annealing techniques will enable us to simulate the various steps of the magnet manufacturing and so reach a better preselection of the LHC strand coating.

ACKNOWLEDGMENT

The authors thank J. Adam, G. Spigo, A. Wilson and R. Wolf for all the fruitful discussions. Special thanks to P. Chevassus, C-H. Denarié, R. Guigue, P-F. Jacquot, J.-L. Servais and J. Stott for their technical support and contribution. The laboratories which have prepared the samples are CERN workshop, Protection Electrolytique des Métaux (France) and GEC Alstom.

REFERENCES

- [1] D. Richter, J. D. Adam, J-M. Depond, D. Leroy, L. R. Oberli, "DC measurement of electrical contacts between strands in superconducting cables for the LHC main magnets", Presented at Applied Superconducting Conference, Pittsburgh, USA, August 25-30, 1996.
- [2] R. Wolf, D. Leroy, D. Richter, A. P. Verweij and L. Walckiers, "Determination of interstrand contact resistance from loss and field measurements in LHC dipole prototypes and correlation with measurements on cable samples", Presented at Applied Superconducting Conference, Pittsburgh, U.S.A., August 25-30, 1996.
- [3] *The Large Hadron Collider - Conceptual Design*, CERN/AC/95-05, 1995.
- [4] J-M. Depond, "Superconducting cable topology," unpublished.
- [5] R. Holm, *Electrical Contacts - Theory and Applications*, 4th ed., Berlin: Springer-Verlag, 1967.
- [6] J. Bénard, *Oxydation des Métaux*, vol. I-II. 1st ed., Paris, Gauthier-Villars, 1962